land

Article

Analysis of Spatial Characteristics Contributing to Urban Cold Air Flow

Hyunsu Kim [1], Kyushik Oh [1,*] and Ilsun Yoo [2]

[1] Department of Urban Planning and Engineering, Hanyang University, Seoul 04763, Republic of Korea; ho1ho1ho2@hanyang.ac.kr
[2] Cheil Engineering Co., Ltd., Seoul 06779, Republic of Korea; ehrtm110@naver.com
* Correspondence: ksoh@hanyang.ac.kr

Abstract: To mitigate the urban heat island phenomenon at night, cool, fresh air can be introduced into the city to circulate and dissipate the heat absorbed during the day, thereby reducing high urban air temperatures. In other words, cold air flow (CAF) generated by mountainous and green areas should be introduced to as wide an area as possible within the city. To this end, it is necessary to first understand the characteristics of urban spatial factors that impact CAF, and to conduct concrete and quantitative analyses of how these urban spatial characteristics are contributing to air temperature reduction. In this study, the following are conducted: (1) an analysis of the relationship between cold air volume flux (CAVF) and the amount of air temperature reduction; (2) urban spatial categorization; (3) an analysis of the relationship between CAVF and the amount of air temperature reduction by urban spatial type; (4) a regression analysis between the amount of air temperature reduction and urban spatial characteristic factors that affect CAF; and finally, (5) the use of CAF to reduce urban air temperatures in urban planning and a design is proposed. Urban space was categorized into nine types using the results of the tertile analysis of CAVF and urban temperature reduction. It was determined that building height (BH) has a positive (+) influence on all urban spatial types, while building area ratio (BA) has a negative (−) effect. However, in the case of wall area index (WAI), the direction of influence varied depending on the development density; relatively low BA areas should focus on development that increases height to increase WAI, while relatively high BA areas should focus on development that reduces BA to reduce WAI by targeting development types closer to the tower type. And even in areas with similar development density, influence varies depending on the terrain elevation. Moreover, it is necessary to prepare improvement measures to increase the factors with CAF that positively influence air temperature reduction and decrease those with negative influence according to the characteristics of urban spatial types. Such results quantitatively and specifically confirmed the effects of spatial factors that affect CAF by urban spatial type on air temperature reduction. The results of this study can be used as useful information for the efficient use of CAF, a major element of urban ecosystem services.

Keywords: urban spatial characteristics; cold air flow; air temperature reduction; urban heat island; urban planning

check for updates

Citation: Kim, H.; Oh, K.; Yoo, I. Analysis of Spatial Characteristics Contributing to Urban Cold Air Flow. *Land* **2023**, *12*, 2165. https://doi.org/10.3390/land12122165

Academic Editors: Alessio Russo and Giuseppe T. Cirella

Received: 13 October 2023
Revised: 7 December 2023
Accepted: 11 December 2023
Published: 14 December 2023

1. Introduction

Urban heat islands are a representative environmental problem caused by rapid urbanization, where the air temperature of areas within a city is approximately 2K–3K higher than that of suburban areas [1]. The rapid urbanization substantially reduces the volume of the natural space of the urban ecosystem services within them, leading to stronger heat island intensities. For example, increased sensible and storage heat due to increased buildings, artificial heat emissions from human activities, and reduced evapotranspiration potential due to decreased vegetation and increased impervious surfaces have been identified as the primary causes of the urban heat island phenomenon [1–5]. In particular, closed urban spaces developed in high-rise and high-density areas block the circulation and inflow of air in the city, which worsens natural ventilation [6,7]. Furthermore, the heat stored in the urban fabric inside the city during the day cannot escape, causing the urban heat island phenomenon to continue even after sunset.

To mitigate the aforementioned urban heat island phenomenon at night, cool and fresh air can be transported into the city to circulate and dissipate the heat absorbed during the day, thereby reducing high urban air temperatures [8–14]. Cold air is generated by radiative cooling of surfaces, which initiates the transport of sensible heat from the air to the surface. Cold air flows (CAF) are driven by differences in air temperature and pressure [15–18]. This flow of cool, fresh air is defined as CAF [19], and it can be used to transport cool, fresh air generated in mountainous and green areas into the city while dissipating heat within.

CAF is generated between sunset and sunrise when the atmospheric temperature decreases due to decreased solar radiant energy [20], mainly in mountainous and green areas, and flows into the city with atmospheric currents at night. Several studies have been conducted to materialize the concept of CAF, focusing on the path and cold air volume flux (CAVF) generated by mountainous and green areas around cities and using them in urban planning and design [21–26]. Such studies emphasized that CAF can be effectively used to improve the thermal environment of urban spaces. In addition, there have been many studies that have simulated the impact of CAF on mitigating the urban thermal environment. In other words, it is necessary to devise specific measures to enable CAF generated by mountainous and green areas to reach the widest areas possible within the city [17,27,28].

However, from an urban planning and design perspective, there is still a lack of research on how the physical characteristics of urban spaces, such as the path of CAF from its entry into the city to its dissipation and the amount of CAF, can be used to reduce urban air temperatures. Additionally, efforts are needed to apply the flowing principles of CAF to urban planning and design based on scientific and quantitative analysis. To this end, it is necessary to first understand the characteristics of urban spatial factors that impact CAF, and to conduct concrete and quantitative analyses of how these urban spatial factors are contributing to air temperature reduction by urban spatial type. It is possible to establish a space-specific customized cold air supply plan based on characteristic analysis and analysis of cold air hindrances for each urban space. Ultimately, urban planning and design for urban air temperature reduction using cold air will be possible [25,27,29]. Thus, in this study, the relevance of CAVF that can be advected into urban spaces to the amount of air temperature reduction is analyzed. Second, the urban space is categorized according to a combination of CAVF and the amount of urban temperature reduction. Third, the relationship between the CAVF and the amount of temperature reduction for each urban spatial type is analyzed, along with the contribution of urban spatial characteristics that help CAF lead to urban air temperature reduction. Finally, based on the analysis results, a plan to use CAF to reduce urban air temperature in urban planning and a design are proposed.

2. Materials and Methods

The study has been conducted in the following steps (Figure 1): (1-1) Analysis of CAVF; (1-2) Identification of urban air temperature and amount of air temperature reduction; (2) Analysis of the relationship between CAVF and amount of air temperature reduction; (3) Categorization of urban spatial type considering CAVF and amount of air temperature reduction; (4) Analysis of the relationship between CAVF and the amount of air temperature reduction by urban spatial type; (5) Regression analysis between the amount of air temperature reduction and urban spatial characteristic factors that affect CAF by urban spatial type; and (6) Derivation of urban spatial characteristic factors as well as urban planning and design implications by urban spatial type.

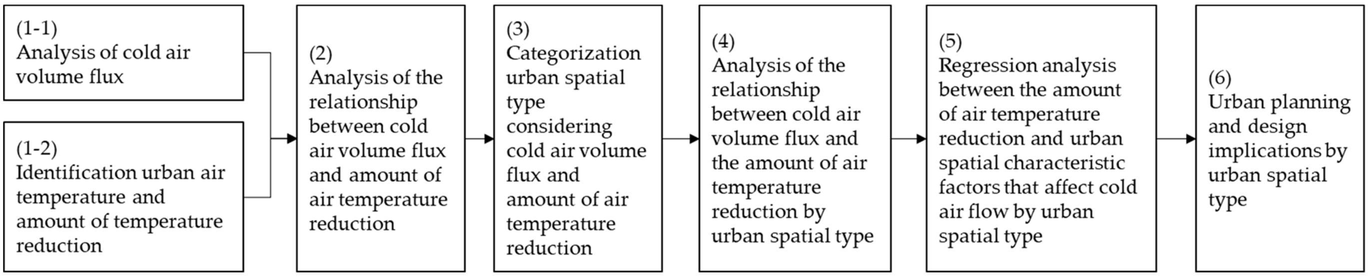

Figure 1. Study workflow.

A case study was carried out for Seoul, the capital and largest city in South Korea (Figure 2). Seoul is located in a temperate climate, is one of the most densely populated cities in the world, and is home to about 18.5% of the total population (approximately 9.5 million people). Seoul is a heat island city characterized by very high-density development.

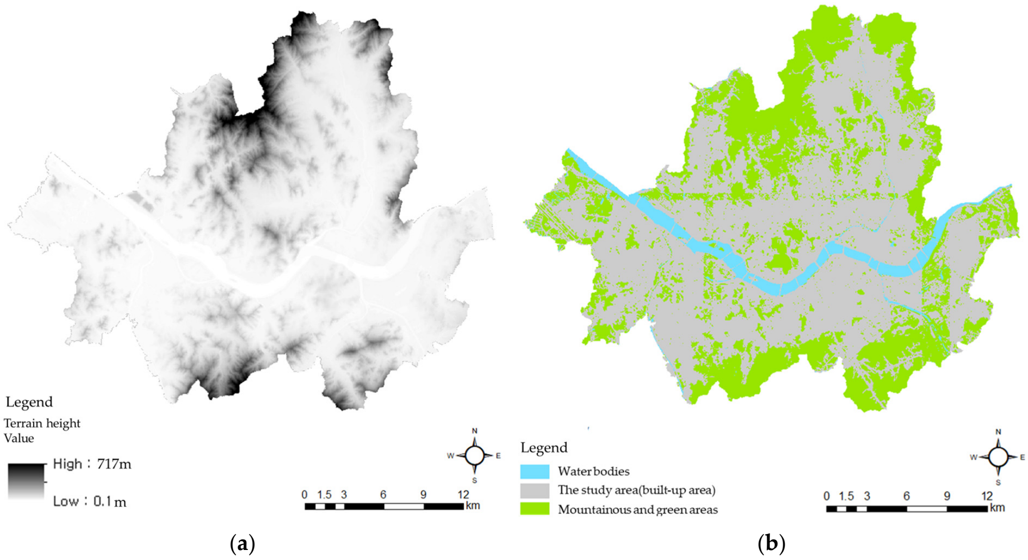

Figure 2. Terrain height (**a**) and land cover (**b**) in the study area (Seoul, Republic of Korea).

In this study, an analysis on the CAVF was performed with a 50 m × 50 m resolution, considering KLAM_21 modeling resolution. As the purpose of this study is to analyze the relationship between the CAVF and air temperature reduction in urban spaces and to identify CAF-influenced urban spatial characteristics that can reduce urban air temperature, a total of 50,950 grids (127.4 km^2) were used for analysis after excluding spaces that generate CAF such as water bodies (e.g., rivers and streams), mountainous areas, and green areas.

2.1. CAVF and the Amount of Urban Air Temperature Reduction

2.1.1. CAVF

There are four main methods for analyzing the CAF, namely, physical measurements, numerical modeling analysis, wind tunnel testing, and using theoretical analysis (Table 1). When using theoretical analysis for CAF analysis, the empirical constants required for the analysis may be inappropriate for the circumstances of the case study area [19]. There are several limiting factors while analyzing the CAF through physical measurements, such as limited observation points (point measurements), time, equipment, cost, and unpredictability. Furthermore, for the wind tunnel tests, scale models of real urban terrain were built, and artificial winds were applied to observe wind flow over terrain and urban structures. However, wind tunnel tests are not suitable for large cities such as Seoul. Alternatively, the analysis of the CAF using numerical models can reflect the urban spatial characteristics of the case study area.

Table 1. Analysis method of CAVF.

		Advantages	Disadvantages
Physical measurements		• Actual measured values • Complex terrain analysis possible	• Incurs installation and maintenance costs • Limited analysis scope • Unable to identify cold air source points
Wind tunnel testing		• Creating a scaled-down model of the actual terrain for wind environment analysis	• Unable to determine the presence of cold air currents • Mainly analyzes changes in wind environment such as building wind due to changes in air flow characteristics, and macro-scale analysis is not possible
Theoretical analysis		• Very straightforward analysis • It is possible to estimate the amount of cold air generation	• Unable to consider actual regional conditions • Macro-scale analysis not feasible
Numerical modeling analysis	KLAM_21	• Specialized simulation analysis for cold air flow, generation, and prediction • Analyzes large-scale areas up to 37.5 × 37.5 km^2 • Reflects actual urban information based on land use	• Unable to analyze temperature
	Envi-met	• Considers surface, vegetation, atmospheric environment, etc., comprehensively • Micro-scale analysis possible • Considers various environmental factors such as temperature, humidity, airflow, plant heat emission, and reflection	• Macro-scale analysis not feasible • Cold air flow analysis is not possible (focused on wind environment changes)
	MUKLIMO_3	• Analyzes wind flow considering terrain, buildings, vegetation, etc. • Micro-scale wind flow simulation possible	• Macro-scale analysis not feasible • Cold air flow analysis is not possible (focused on wind environment changes)

Representative numerical modeling programs to analyze CAF include KLAM_21, Envi-met, MUKLIOMO_3, REWIMET, and FITNAH. Among various numerical modeling programs, for this study, KLAM_21 Version 2.012 was applied to analyze CAF by considering various conditions such as the possibility of analyzing at the scale of a large city like Seoul, the case study area, the possibility of considering various land uses, and the possibility of high-resolution analysis. KLAM_21 is a modeling analysis tool for the CAVF developed by the German Meteorological Service (DWD, Deutscher Wetterdienst). KLAM_21 can be operated with up to 3000 × 3000 grid cells, and each grid can be analyzed with a resolution of 10–50 m [23].

For KLAM_21 modeling, elevation and land use-specific physical parameters are required. Physical parameters include roughness, building coverage area ratio (BA), building height (BH), wall area index (WAI), tree cover fraction, tree height, leaf area index (LAI), and local heat loss rate. It is important to accurately determine the parameter values depending on the properties of the case study area. However, because the appropriate parameters have not yet been established for Seoul, it was necessary to construct physical parameters that fit the characteristics of the case study area. For the modeling analysis, a spatial scope of analysis with a 50 × 50 m grid resolution was considered and physical parameters for the analysis were prepared using GIS spatial analysis (Table 2 and Figure A2). The KLAM_21 modeling run time was set from 9 p.m. (sunset) to 6 a.m. (sunrise), which is the time when cold air is generated in mountainous and green areas after sunset. A map of the CAVF from 9 p.m. to 6 a.m. was prepared.

Table 2. KLAM_21 modeling Physical Parameters.

Class	Z0	BA	BH	WAI	TA	TH	LAI	α
Forest	0.4	-	-	-	0.4	13.8	3.5	0.56
Semi-sealed	0.02	-	-	-	-	-	-	0.64
Industrial	0.08	0.3	6.3	1.34	-	-	-	0
Park	0.1	-	-	-	0.3	11	3.0	1.0
Open Space	0.05	-	-	-	-	-	-	1.0
Sealed	0.01	-	-	-	-	-	-	0.28
Water	0.001	-	-	-	-	-	-	0
Low rise (1–3 floors) 3–9 m	0.1	0.21	5.71	1.98	0.0	0.0	0.0	0.28
Low–mid rise (4–8 floors) 10–26 m	0.1	0.34	10.42	3.36	0.0	0.0	0.0	0.28
Mid rise (9–16 floors) 27–48 m	0.1	0.2	39.54	8.16	0.0	0.0	0.0	0.0
Mid–high rise (17–26 floors) 49–78 m	0.3	0.2	62.91	12.88	0.0	0.0	0.0	0.0
High rise (27–123 floors) 79–555 m	0.3	0.23	103.2	15.6	0.0	0.0	0.0	0.0

Z0: roughness length (m), BA: building coverage area ratio, BH: building height (m), WAI: wall area index, TA: tree cover fraction, TH: mean tree height (m), LAI: leaf area index, and α: relative local heat loss.

2.1.2. Urban air Temperature and Amount of Air Temperature Reduction

The urban heat island phenomenon is typically most pronounced two to three hours after sunset on cloudless and calm days [1]. The analysis time in this study considered these characteristics of urban heat islands. Eight days in the summer of 2021 were selected considering the weather conditions (cloud cover of at most 5/8), low wind speed ($\leq$2 m/s)) and KLAM_21 modeling analysis time (9 p.m. to 6 a.m.) (Table 3).

An air temperature map was prepared by using weather data collected from 26 Automatic Weather Stations (AWS) operated by the Korea Meteorological Administration (KMA) and about 1100 Smart City Data Sensors (S-dot) operated by the Seoul Metropolitan Government (Figure 3). In this study, the universal kriging interpolation method was applied based on the Gaussian process regression model [30] to consider the variables of distance between measurement points, altitude, and distance to the river. Air temperature maps at 9 p.m. and 6 a.m. for eight days in the summer of 2021 on a 50 m × 50 m resolution grid were produced. Finally, the difference between the 9 p.m. and 6 a.m. air temperatures was calculated to create a mean urban air temperature reduction map.

Table 3. Time of analyzing urban air temperatures.

	Minimum Air Temperature (°C)	Maximum Air Temperature (°C)	Mean Air Temperature (°C)	Mean Wind Speed (m/s)	Mean Cloud Cover
9 June 2021	19.5	31.6	25.8	1.6	3.4
13 June 2021	20.9	29.7	24.8	2.0	3.5
1 July 2021	21.4	31.0	26.3	1.8	2.3
21 July 2021	25.3	35.3	30.5	1.7	3.5
23 July 2021	27.2	35.8	31.2	1.8	2.3
24 July 2021	26.9	36.5	31.7	1.7	3.0
28 July 2021	27.1	34.7	30.4	1.8	3.6
7 August 2021	23.4	32.3	28.0	2.0	3.3

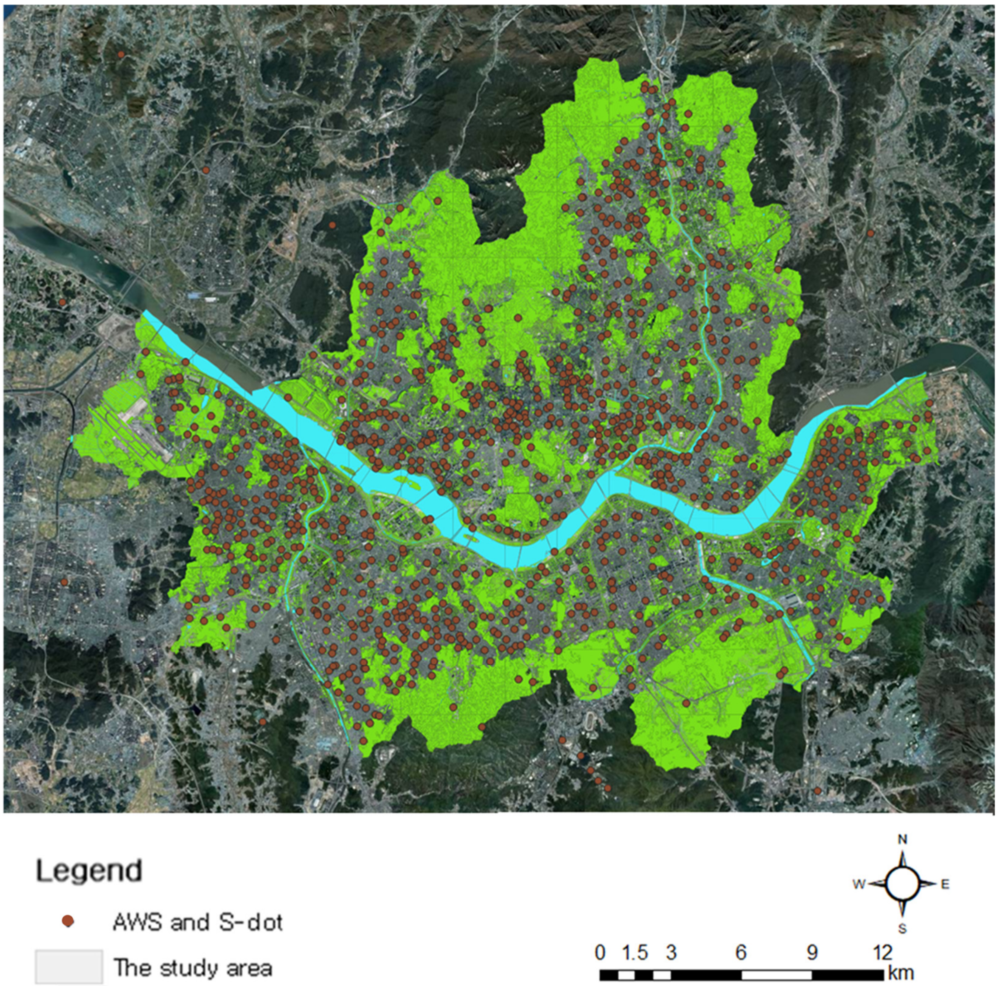

Figure 3. AWSs and S-dot sensors in the study area.

2.2. Analysis of the Relationship between the CAVF and the Amount of Urban Air Temperature Reduction

To examine the relationship between CAVF and the amount of air temperature reduction in the case study area, correlation analysis was conducted between CAVF and the amount of air temperature reduction. This is to confirm the contribution of CAF generated from mountainous and green areas in the study area to air temperature reduction.

2.3. Urban Spatial Categorization

A city made up of many different spatial factors will have different amounts of CAF and air temperature reduction depending on the characteristics of the spaces. Therefore, in order to categorize urban spaces, it is necessary to classify them according to the CAVF and amount of air temperature reduction. The results of the CAF modeling analysis and the urban air temperature reduction amount calculations were classified into tertile (high, medium, and low) using the Natural Breaks Jenk function (Figure 4). Consequently, the urban spaces were categorized into nine areas as follows: areas with the highest, medium, and lowest CAVF, and areas with the highest, medium, and lowest amount of urban air temperature reduction. Next, the characteristics of each space were identified based on the classified urban spatial categories.

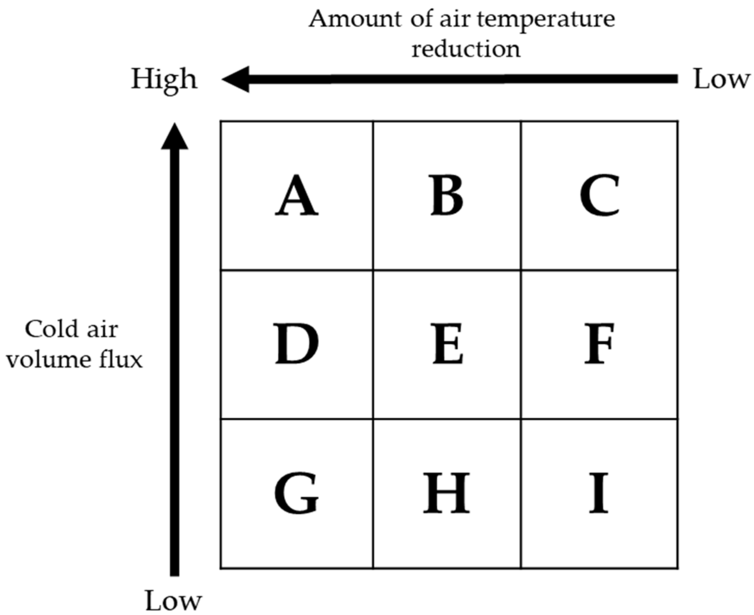

Figure 4. Urban spatial categorization method.

2.4. Identification of Urban Air Temperature Reduction Factors by Urban Spatial Type

Correlation analysis was performed to analyze the relationship between the CAVF and the amount of urban air temperature reduction by urban spatial type. Regression analysis was also performed to find the factors influencing CAF that affect air temperature reduction. The independent variables for the regression analysis are elevation, BH, WAI, and BA among the input variables of KLAM_21. The peripheral borders of the mountainous and green areas have cooler air temperatures than built-up areas, so CAF has a less significant effect on air temperature drops. Therefore, distance to green areas and the normalized difference vegetation index (NDVI) were added as independent variables to account for the effect of mountainous areas and green areas. Regression analysis was performed using the standardized values of the variables, and the amount of air temperature reduction was selected as the dependent variable to find the influential variables that affect air temperature reduction. Moreover, the amount of urban air temperature reduction utilizes air temperatures measured by the AWSs and s-dot; as spatial autocorrelation is generally known to exist, this can be problematic for spatial autocorrelation due to the first law of geography [31]. Therefore, spatial autoregressive models (spatial lag model (SLM) and spatial error model (SEM)), which are regression models that control for spatial autocorrelation, were applied.

3. Results

3.1. Analysis Results of the CAVF and the Amount of Urban Air Temperature Reduction

3.1.1. Analysis Results of the CAVF

KLAM_21 was utilized to analyze CAF for a 9 h period from 9 p.m. to 6 a.m., when cold air is generated after sunset (Figure A1). The unit of the CAVF is m^3/ms, which indicates the volume of cold air traveling a unit distance per unit area. As the time passes from after sunset to before sunrise, the CAF generated by the mountainous and green areas entering the city can be detected. Figure 5 is a CAF map that adds all the analysis results for 9 h, excluding water bodies (e.g., rivers and streams), mountains, and green areas of the study area. Many areas are experiencing an inflow of CAF, with a few exceptions. In the north and southeast, where large mountainous regions are located, a relatively smooth CAF can be determined. However, densely developed urban areas, including the southwestern part of the study area, were receiving relatively little CAF. This suggests that some spaces within the study area do not have a smooth CAF within the urban space.

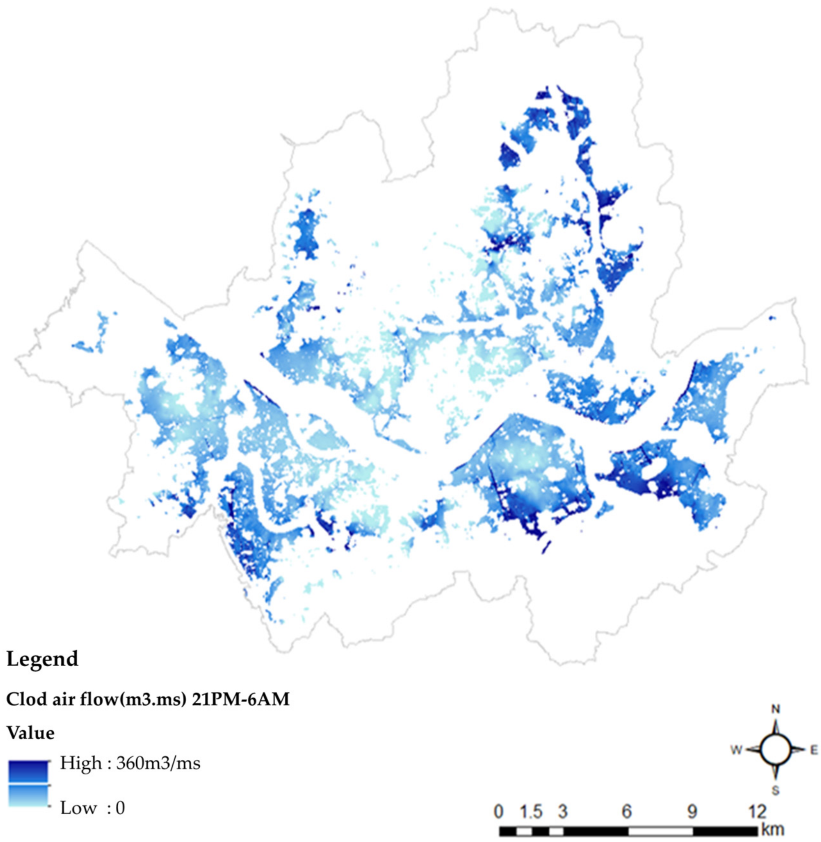

Figure 5. The total CAVF from 9 p.m. to 6 a.m. in the study area.

3.1.2. Analysis Results of Urban Air Temperature and Amount of Air Temperature Reduction

Figure 6 is a map of the air temperature at 9 p.m. and 6 a.m. in the study area. The air temperature at 9 p.m. ranged from 28.6 °C to 34.4 °C with a mean value of 32.8 °C, and the difference between the maximum and minimum temperatures was 5.8 °C. This confirms that the urban heat island phenomenon is severe in the study area. This phenomenon can also be seen in the air temperature distribution map. Higher air temperatures were found in urban areas with relatively high development densities and lower air temperatures were found in the north, east, and south, where large urban forests are predominantly located. At 6 a.m., the air temperature ranged from 25.4 °C to 29.9 °C with a mean value of 28.7 °C. The difference between the maximum and minimum air temperatures was 4.5 °C. The analysis of air temperature reduction between 9 p.m. and 6 a.m. showed that the north and east areas closest to the urban forests experienced a maximum nighttime air temperature reduction of 5.9 °C, while the lowest air temperature difference of 2.3 °C was found in the west area, which has a relatively high development density and no urban forests nearby (Figure 7).

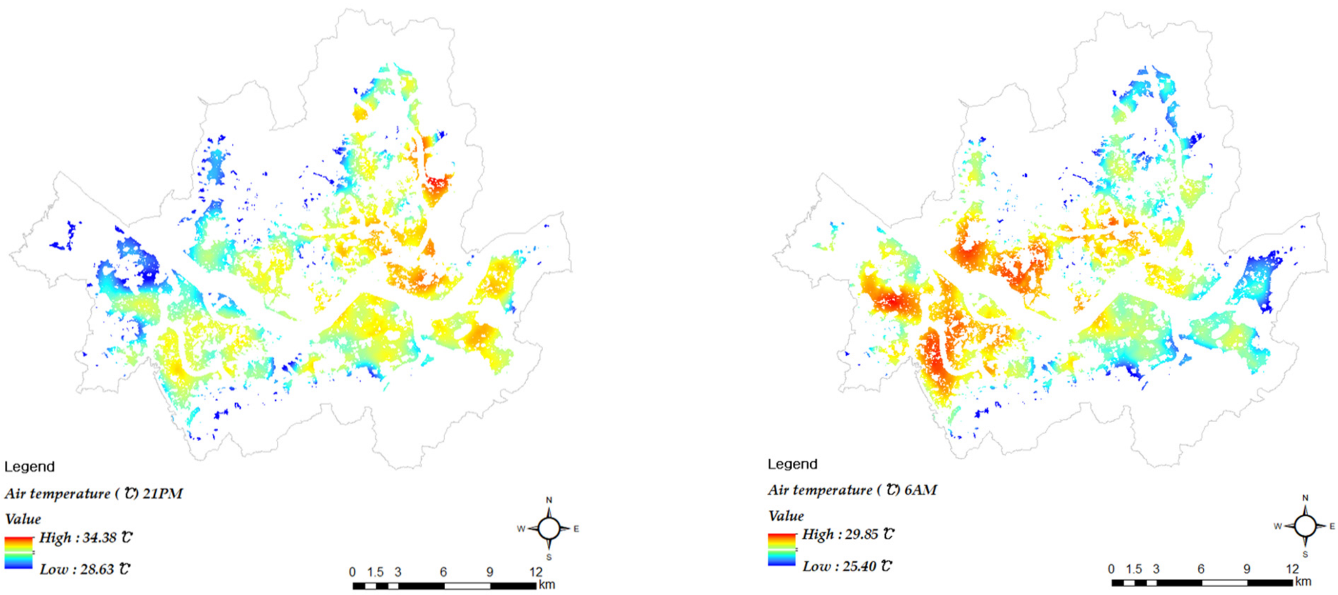

(**a**) (**b**)

Figure 6. Air temperature analysis results: (**a**) left: 9 p.m.; (**b**) right: 6 a.m.

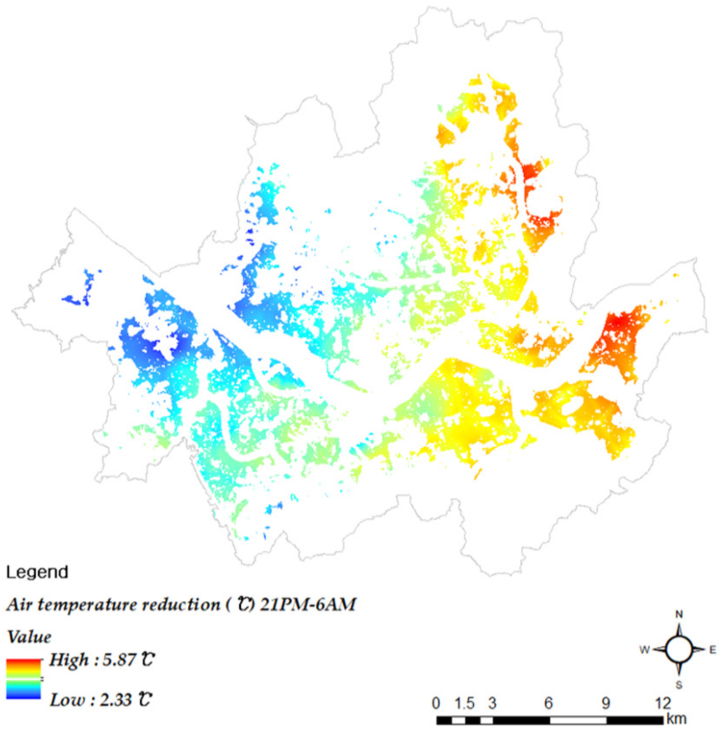

Figure 7. Air temperature reduction analysis (9 p.m.–6 a.m.).

3.2. Analysis Results of the Relationship between the CAVF and The Amount of Urban Air Temperature Reduction

Table 4 shows the results of the correlation analysis between the total CAVF and the amount of air temperature reduction in the study area: the higher the positive correlation coefficient, the greater the air temperature reduction effect of the CAVF. A positive correlation was shown across the study areas, and thus confirms that CAVF contributes to air temperature reduction. This is the result of the analysis of the entire study area. Additional analysis is needed by urban spatial type because the degree to which CAVF contributes to urban temperature reduction will vary depending on the characteristics of urban space.

Table 4. Analysis results of the correlation between the amount of overall CAF and the amount of air temperature reduction across study areas.

		CAVF (Seoul)
Amount of Air temperature Reduction	Pearson Correlation	0.394 **
	N	50,950

** Correlation is significant at the 0.01 level (two-sided).

3.3. Urban Spatial Categorization Results

Using the tertile analysis results of the CAVF and the amount of urban air temperature reduction, the urban spaces of the study areas were categorized into the following nine types: areas with high CAVF and high air temperature reduction (Type A), areas with high CAVF and medium air temperature reduction (Type B), areas with high CAVF and low air temperature reduction (Type C), areas with medium CAVF and high air temperature reduction (Type D), areas with medium CAVF and medium air temperature reduction (Type E), areas with medium CAVF and low air temperature reduction (Type F), areas with low CAVF and high air temperature reduction (Type G), areas with low CAVF and medium air temperature reduction (Type H), and areas with low CAVF and low air temperature reduction (Type I) (Figure 8 and Table 5). The spatial characteristics of each urban spatial type are shown in Table 6. The BH, WAI, and BA were all relatively low for Types A, B, and C, which have more CAF, while Types G, H, and I, which have less CAF, were classified as areas with relatively high BH, WAI, and BA. Except for Types H and G, which are located at high altitudes, the more the CAVF and the amount of air temperature reduction, the greater the distance from green areas, and the higher the BH and WAI. In the case of NDVI, it was similar for all urban spatial types because mountainous and green areas were excluded, which are the source spaces of generating CAF and classified urban spaces. In terms of land use, the lower the CAVF and the amount of air temperature reduction in relatively flat types (except for Types G and H, which have higher elevations and a higher proportion of high-rise residences), the lower the proportion of high-rise residences and commercial/office buildings with higher BH than low-rise residences. The high CAF types (Types A, B, and C) make up only ~12% of the region's total study area. However, Types G, H, and I, which make up about 48% of the study area, showed less CAF and therefore have more potential to utilize CAF to reduce air temperatures than other types. These types of urban spaces are relatively high-rise and densely developed areas. In sum, depending on the elevation and development density in the study area, it is possible to improve urban heat islands by actively considering factors influencing cold air in urban planning and design for a smooth CAF.

Table 5. Urban spatial categorization results.

	Type A (*n* = 4888)	**Type B (*n* = 1167)**	**Type C (*n* = 256)**	**Type D (*n* = 11,475)**	**Type E (*n* = 4798)**	**Type F (*n* = 3769)**	**Type G (*n* = 5516)**	**Type H (*n* = 10,730)**	**Type I (*n* = 8351)**
Elevation	−0.3298	−0.2955	−0.3453	−0.2449	−0.3003	−0.5688	0.4402	0.6715	−0.1429
NDVI	−0.0620	−0.1033	0.5304	−0.0561	−0.1,100	−0.0931	−0.1123	0.1787	0.0613
BH	−0.1288	−0.2675	−0.6371	0.0541	−0.0596	−0.1949	0.0437	0.1522	−0.0443
WAI	−0.1242	−0.3562	−0.8158	0.0788	−0.0863	−0.1624	0.0316	0.1409	−0.0398
BA	−0.2603	−0.2610	−0.5723	−0.1318	0.1296	0.0284	0.0522	0.0105	0.0665
Distance to green areas	0.0358	−0.0065	−0.4046	0.1074	0.0635	0.0450	0.2597	−0.3434	0.1151

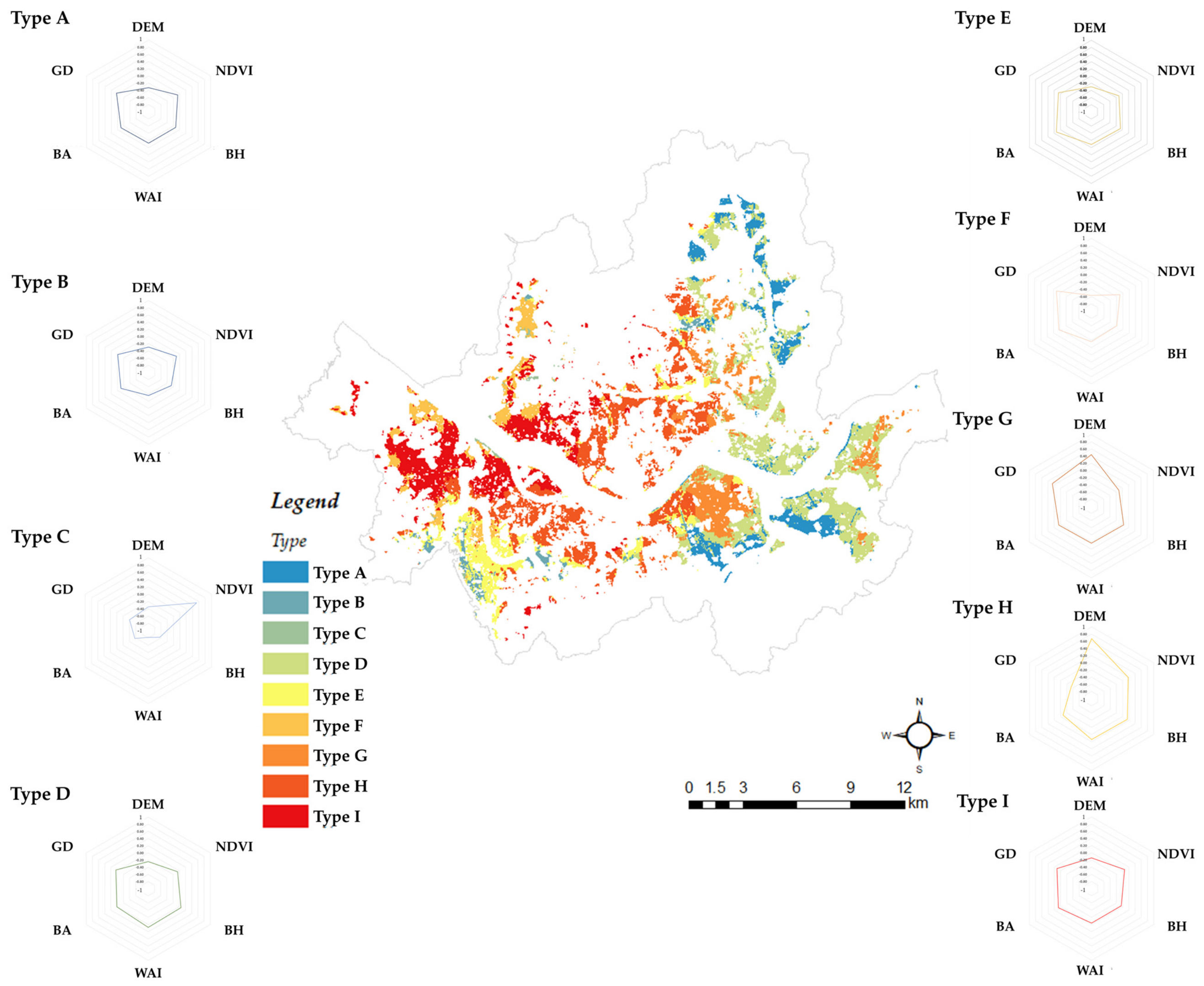

Figure 8. Urban spatial categorization results.

Table 6. Spatial characteristics by urban spatial type.

		CAVF	Amount of Air Temperature Reduction	Elevation	NDVI	BH	WAI	BA	Distance to Green Areas	Land Use (%)
Type A (*n* = 4888)	Max	359.99	5.85	51	0.42	165	24.95	1	1104.54	Low-rise residential: 34.39
	Min	63.82	4.43	10	−0.01	0	0	0	0	Road: 23.85
	Mean	84.11	4.95	19.97	0.14	18.69	4.64	0.25	360.88	High-rise residential: 20.50
	S.D.	24.50	0.30	6.80	0.07	17.86	3.24	0.18	206.08	Commercial: 14.92
Type B (*n* = 1167)	Max	256.62	4.43	71	0.42	87	22.02	0.96	806.22	Low-rise residential: 28.61
	Min	63.82	3.59	0	0.01	0	0	0	0	Road: 24.65
	Mean	84.02	3.93	20.66	0.13	15.93	3.80	0.25	352.29	High-rise residential: 13.90
	S.D.	30.04	0.23	14.10	0.07	17.26	3.61	0.22	198.36	Commercial: 10.31
Type C (*n* = 256)	Max	289.02	3.59	81	0.43	48	10.97	0.92	860.23	Low-rise residential: 30.88
	Min	63.82	2.76	7	0.03	0	0	0	0	Road: 24.57
	Mean	82.39	3.24	19.66	0.16	8.58	2.13	0.20	271.37	Open space: 17.28
	S.D.	26.80	0.23	14.47	0.09	10.68	2.18	0.22	220.24	Commercial: 6.46

Table 6. *Cont.*

		CAVF	Amount of Air Temperature Reduction	Elevation	NDVI	BH	WAI	BA	Distance to Green Areas	Land Use (%)
Type D (*n* = 11,475)	Max	63.81	5.87	60	0.47	174	27.37	1	1204.16	Low-rise residential: 40.37
	Min	28.39	4.43	10	−0.01	0	0	0	0	High-rise residential: 21.82
	Mean	44.34	4.94	21.67	0.14	22.33	5.37	0.27	375.42	Road: 16.43
	S.D.	9.90	0.31	8.61	0.06	21.26	3.89	0.16	203.42	Open space: 12.25
Type E (*n* = 4798)	Max	63.81	4.43	82	0.47	123	21.54	1	860.23	Low-rise residential: 40.58
	Min	28.39	3.59	5	−0.02	0	0	0	0	Road: 17.73
	Mean	42.11	3.91	20.56	0.13	20.07	4.77	0.32	366.50	High-rise residential: 17.40
	S.D.	9.69	0.23	11.88	0.06	18.91	3.46	0.18	187.12	Commercial: 12.69
Type F (*n* = 3769)	Max	66.75	3.59	83	0.52	108	20.22	0.99	948.68	Low-rise residential: 41.76
	Min	28.39	2.53	7	−0.01	0	0	0	0	Road: 18.39
	Mean	40.13	3.21	15.17	0.13	17.38	4.50	0.31	362.75	High-rise residential: 15.44
	S.D.	8.96	0.21	8.16	0.06	14.99	2.88	0.17	197.90	Commercial: 9.82
Type G (*n* = 5516)	Max	28.39	5.68	129	0.49	162	23.87	1	1204.16	Low-rise residential: 40.57
	Min	0	4.43	11	−0.03	0	0	0	0	High-rise residential: 16.83
	Mean	17.26	4.76	35.42	0.13	22.12	5.20	0.31	406.38	Commercial: 16.77
	S.D.	8.54	0.26	16.68	0.07	19.28	3.61	0.16	246.66	Road: 13.36
Type H (*n* = 10,730)	Max	28.37	4.43	233	0.48	207	26.46	1	860.23	Low-rise residential: 40.88
	Min	0	3.59	6	−0.02	0	0	0	0	High-rise residential: 24.58
	Mean	17.08	3.99	40.06	0.15	24.28	5.59	0.30	283.81	Commercial: 12.24
	S.D.	9.18	0.25	27.45	0.07	22.28	3.94	0.17	160.26	Road: 13.64
Type I (*n* = 8351)	Max	28.38	3.59	293	0.49	207	26.15	1	1019.80	Low-rise residential: 44.38
	Min	0	2.33	6	−0.02	0	0	0	0	High-rise residential: 17.27
	Mean	14.90	3.22	23.72	0.14	20.37	4.94	0.31	377.00	Commercial: 13.09
	S.D.	8.08	0.25	24.34	0.07	18.28	3.23	0.17	207.46	Road: 15.94

3.4. Results of Identifying Urban Air Temperature Reduction Factors by Type of Urban Space

Table 7 shows the results of the correlation analysis between the CAVF and the amount of air temperature reduction by urban spatial type. The higher the positive correlation coefficient, the more the CAVF contributes to the air temperature reduction. A positive correlation was found across all urban spatial types. The higher the air temperature reduction (Type A and D), the stronger the positive correlation, while the lower the air temperature reduction or the lower the CAVF, the lower the positive correlation. Areas with a higher positive correlation tend to be located on flat land, far from green areas, and show a development form with relatively high BH and WAI.

Table 7. Correlation of the CAVF and the amount of air temperature reduction by urban spatial type.

		CAVF								
		Type A	Type B	Type C	Type D	Type E	Type F	Type G	Type H	Type I
Amount of air temperature reduction	Pearson Correlation	0.481 *	0.407 *	0.326 *	0.511 *	0.491 *	0.366 *	0.333 *	0.344 *	0.350 *
	N	4888	1167	256	11,475	4798	3769	5516	10,730	8351

* Correlation is significant at the 0.01 level (two-sided).

Table A1 shows the regression analysis results of the amount of air temperature reduction and factors influencing CAVF by urban spatial type. Among the three regression models, the SEM model was found to have the highest log likelihood value, which indicates high suitability. In the SEM, all six independent variables were significant at the 1% level. Analysis results of SEM revealed the six variables can be categorized into natural and artificial factors based on whether they can be manipulated in urban planning and design.

The natural factors are elevation, NDVI, and distance to green areas, and the artificial factors are BH, WAI, and BA. The absolute values of the coefficients of the independent variables in all urban spatial types were higher in the order of elevation, distance to green areas, and NDVI for natural factors, and higher in the order of BH, WAI, and BA for artificial factors. However, the signs of the coefficients of the independent variables were analyzed differently for each type of urban space. Elevation, NDVI, and distance to green areas showed positive signs for all urban spatial types. BH showed a positive sign for all urban spatial types, and BA showed a negative sign for all urban spatial types. However, the effects of WAI vary depending on elevation and development density. Positive signs were found in areas with relatively low BA, such as Types A, B, C, and D, and in Types G and H with high elevation and BH, while negative signs were found in Types E, F, and I with relatively high BA (Tables 8 and 9).

Table 8. Spatial regression analysis results by urban spatial type.

	Type A	Type B	Type C	Type D	Type E	Type F	Type G	Type H	Type
Elevation	0.015715	0.131069	0.050024	0.02743	0.040678	0.052277	0.04338	0.002747	0.00667
NDVI	0.00097	0.00289	0.005849	0.000958	0.00255	0.001553	0.001692	0.00017	0.00132
BH	0.00361	0.01382	0.092827	0.00785	0.00067	0.013152	0.008919	0.00045	0.002249
WAI	0.005989	0.009598	0.05023	0.005491	−0.00054	−0.01139	0.003234	0.00032	−0.00253
BA	−0.001165	−0.00317	−0.01934	−0.000825	−0.00028	−0.0012	−0.00105	−0.00032	−0.0008
Distance to green areas	0.01227	0.011781	0.005794	0.007555	0.007517	0.02466	0.034309	0.00559	0.012248
Constant term	1.05584	−0.33896	−1.18172	0.949379	−0.29672	−1.23183	0.885141	−0.30435	−1.2174
Log likelihood	5733.09	1211.93	168.69	18154.13	6677.75	5592.04	7799.59	17207.67	13935.50
R2	0.80	0.75	0.74	0.79	0.78	0.75	0.81	0.78	0.79

Table 9. Relationship between the factors influencing the amount of air temperature reduction and CAF.

	Type A	Type B	Type C	Type D	Type E	Type F	Type G	Type H	Type I
Elevation	+	+	+	+	+	+	+	+	+
NDVI	+	+	+	+	+	+	+	+	+
BH	+	+	+	+	+	+	+	+	+
WAI	+	+	+	+	-	-	+	+	-
BA	-	-	-	-	-	-	-	-	-
Distance to green areas	+	+	+	+	+	+	+	+	+

4. Discussion and Conclusions

The key findings of this study are the following. The analysis of the relationship between the CAVF and the amount of air temperature reduction by urban spatial type showed that the higher the amount of air temperature reduction, the more relevant it is to CAVF (Types A and D). Furthermore, it was found that Type E, which is located in a flat area and has a relatively high BH and WAI, is highly relevant. On the contrary, types with higher elevation (Types G and H) and types with lower proportions of high-rise residences in flat areas (Types F and I) were less relevant. Furthermore, in areas with low BA (Types A, B, C, and D), the relevance of the CAVF and the amount of air temperature reduction varied depending on BH and WAI. The results suggest that elevation, BH, WAI, and BA are the factors in urban planning and design that can reduce urban air temperatures by smoothly enhancing CAF.

Next, the mechanisms through which these factors affect CAF and affect air temperature reduction by urban spatial type were identified. As a result, in urban planning and design, it is necessary to prepare improvement measures for increasing the factors with CAF that positively (+) influence air temperature reduction and decreasing those with negative (−) influence according to the characteristics of urban spatial types. BH had a positive (+) influence on all urban spatial types, and the absolute influence of WAI and BA was a larger factor. BA had a negative (−) influence on all urban spatial types. The higher the height of the building and the lower the BA, the more unimpeded the CAF, maximizing the air temperature reduction effect. However, in the case of the WAI, it needs to be applied differently depending on the development density. Relatively low BA areas (Types A, B, C, and D) should focus on development that increases height to increase WAI, while relatively high BA areas (Types E and F) should focus on development that reduces BA to reduce WAI by targeting development types closer to the tower type. Even in neighborhoods with similar development densities, the impact of development density varies by elevation. Thus, it is possible to ensure smooth CAF as well as the continuity of cold air by providing the direction for improvement based on the characteristics of urban spatial types.

This study has quantitatively analyzed the relationship between the CAVF and the amount of air temperature reduction by urban spatial type, and proposed measures to improve the urban heat island through smooth CAF. The analysis showed that a combination of factors, such as elevation, BH, WAI, and BA, should be considered. The preceding research has mainly focused on the formation and movement of CAF due to natural factors [24,32–34]. However, this study has a significant advantage in focusing on the movement of CAF and temperature reduction caused by physical factors in urban spaces. Additionally, employing a statistical approach enables the confirmation of the influence of physical factors in urban spaces on temperature reduction in a more scientific and quantitative manner, providing practical information for urban planning and design. In particular, when making plans to mitigate the urban heat island phenomenon in large cities such as Seoul, where various urban spaces exist in a complex manner, it is possible to enhance the efficiency of such plans by identifying the factors that hinder CAF in detail through a spatially customized approach. If the smooth CAF can be maintained within the city while simultaneously increasing the inflow of CAF through the strengthening of mountainous and green areas around the city, which serve as resources for urban ecosystem services, a great synergy will be achieved in the circulating and cooling of heat in the city. These implications will provide useful information for the efficient use of CAF, a major element of urban ecosystem services.

This study has the following limitations. Among the physical characteristics of various urban spaces, the analysis focused on factors influencing CAF in KLAM_21. A more comprehensive consideration and analysis of other urban spatial physical characterization variables that were not considered in this study, such as sky view factor (SVF), height to road width (H/W) ratio, and porosity, is needed to determine the exact relationship between factors influencing the amount of urban air temperature reduction and CAF. Furthermore, since there is the limitation of not comprehensively considering both natural and physical factors in urban spaces that contribute to the formation and movement of CAF, future research should involve a more comprehensive and holistic investigation that takes into account both of these factors.

Author Contributions: This article is the result of joint work by all the authors. K.O. supervised and coordinated work on the paper. Conceptualization, K.O. and H.K.; methodology, K.O. and H.K.; validation, K.O. and H.K.; formal analysis, H.K.; data curation, H.K. and I.Y.; writing—original draft preparation, H.K.; writing—review and editing, K.O. and H.K.; visualization, H.K.; supervision, K.O.; project administration, K.O.; funding acquisition, K.O. All authors have read and agreed to the published version of the manuscript.

Funding: This research was funded by the Korea Ministry of Environment (MOE) grant number 2022003570004.

Data Availability Statement: The data presented in this study are available on request from the corresponding author. The data are not publicly available due to an ongoing study.

Acknowledgments: This work was supported by Korea Environment Industry & Technology Institute (KEITI) through "Climate Change R&D Project for New Climate Regime", funded by Korea Ministry of Environment (MOE) (2022003570004).

Conflicts of Interest: Author Ilsun Yoo was employed by the company Cheil Engineering Co., Ltd. The remaining authors declare that the research was conducted in the absence of any commercial or financial relationships that could be construed as a poten-tial conflict of interest.

Appendix A

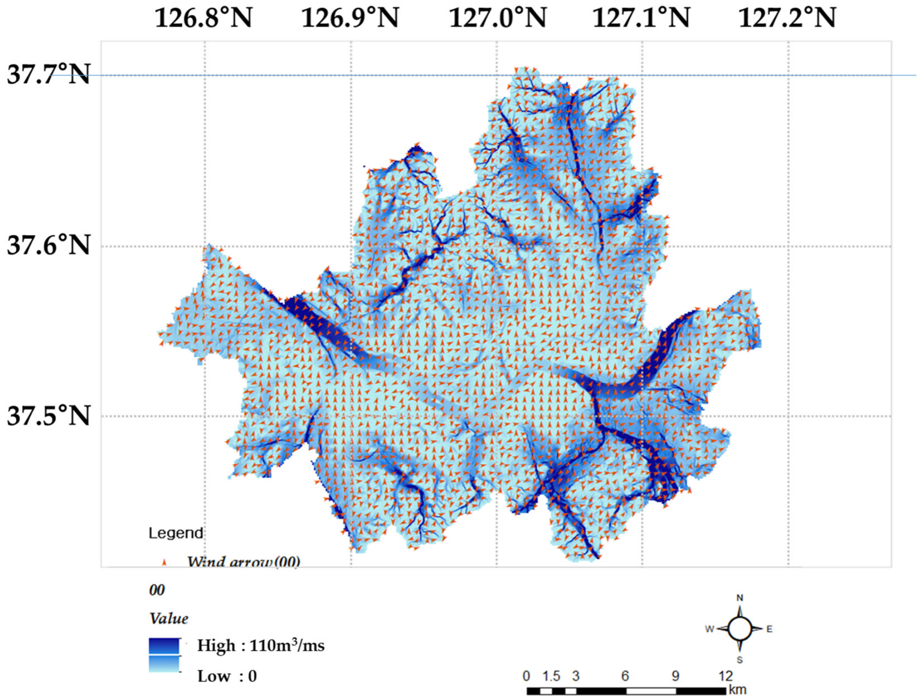

0 a.m.

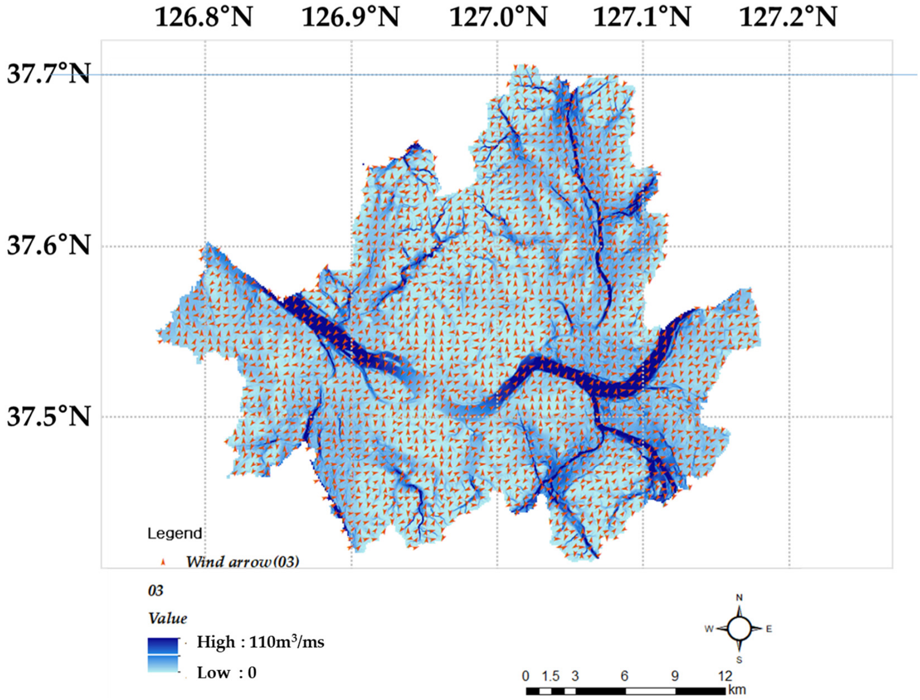

3 a.m.

Figure A1. *Cont*.

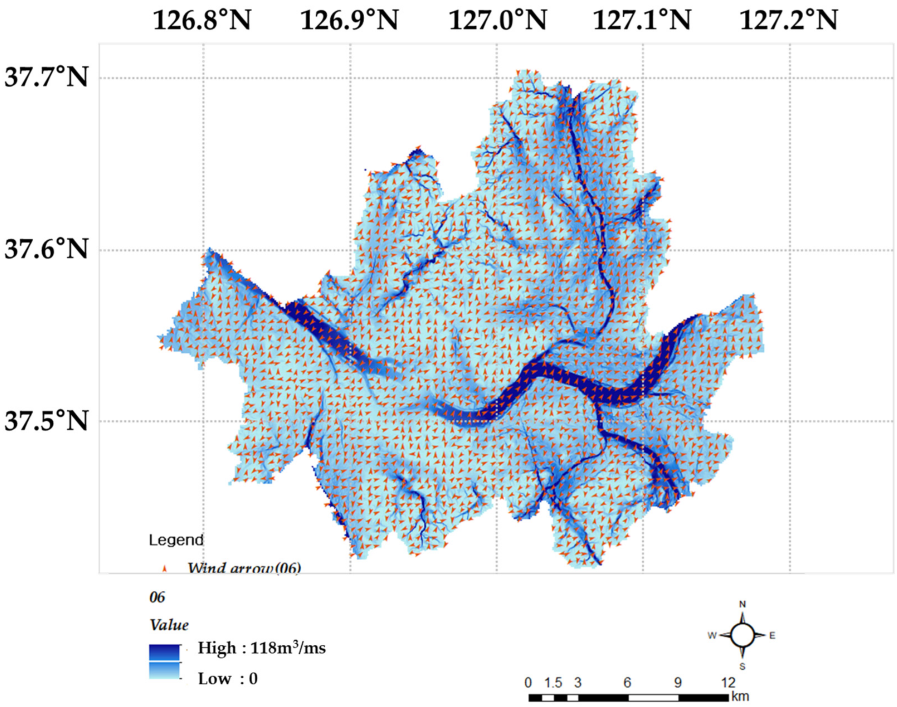

6 a.m.

Figure A1. The CAVF from 0 a.m., 3 a.m. and 6 a.m.

Table A1. Regression analysis results between air temperature reduction and the factors influencing CAF.

		OLS	SLM	SEM
Type A (n = 4888)	Elevation	0.009527	0.02162880987	0.015715
	NDVI	0.013	0.001732	0.00097
	BH	0.20824	0.04015	0.00361
	WAI	0.132445	0.021205	0.005989
	BA	0.001273	−0.0059	−0.001165
	Distance to green areas	0.03936	0.00844	0.01227
	Constant term	1.0414	0.177992	1.05584
	Log likelihood	−2423.76	2009.12	5733.09
	R2	0.26	0.78	0.80
Type B (n = 1167)	Elevation	0.138952	0.020185	0.131069
	NDVI	0.01851	0.00643	0.00289
	BH	0.16345	0.03621	0.01382
	WAI	0.1733	0.035978	0.009598
	BA	−0.01419	−0.00265	−0.00317
	Distance to green areas	0.05924	0.00775	0.011781
	Constant term	−0.29121	−0.05245	−0.33896
	Log likelihood	−83.25	897.92	1211.93
	R2	0.30	0.71	0.75
Type C (n = 256)	Elevation	0.005751	0.03205	0.050024
	NDVI	0.03912	0.03373	0.005849
	BH	0.201706	0.128547	0.092827
	WAI	0.02889	0.04067	0.05023
	BA	−0.047697	−0.030245	−0.01934
	Distance to green areas	0.025339	0.020728	0.005794
	Constant term	−1.12038	−0.80723	−1.18172
	Log likelihood	−20.19	35.69	168.69
	R2	0.32	0.62	0.74

Table A1. *Cont.*

		OLS	SLM	SEM
Type D (n = 11475)	Elevation	0.06705	0.00033	0.02743
	NDVI	0.00024	0.001853	0.000958
	BH	0.11839	0.00822	0.00785
	WAI	0.112607	0.006854	0.005491
	BA	0.033998	−0.000955	−0.000825
	Distance to green areas	0.01465	0.00146	0.007555
	Constant term	1.0155	0.090324	0.949379
	Log likelihood	−6396.11	8789.41	18154.13
	R2	0.22	0.75	0.79
Type E (n = 4798)	Elevation	0.163369	0.00918	0.040678
	NDVI	0.03471	0.00443	0.00255
	BH	0.02464	0.00271	0.00067
	WAI	0.017313	−0.003426	−0.00054
	BA	−0.03298	−0.00161	−0.00028
	Distance to green areas	0.006601	0.002262	0.007517
	Constant term	−0.31871	−0.02243	−0.29672
	Log likelihood	−1035.19	5767.68	6677.75
	R2	0.11	0.67	0.78
Type F (n = 3769)	Elevation	0.163246	0.009748	0.052277
	NDVI	0.04314	0.010399	0.001553
	BH	0.08502	0.01537	0.013152
	WAI	−0.06946	−0.00863	−0.01139
	BA	−0.005411	−0.00659	−0.0012
	Distance to green areas	0.056493	0.019646	0.02466
	Constant term	−1.22814	−0.35632	−1.23183
	Log likelihood	−490.66	1989.70	5592.04
	R2	0.20	0.69	0.75
Type G (n = 5516)	Elevation	0.04289	0.01055	0.04338
	NDVI	0.050936	0.011022	0.001692
	BH	0.02006	0.00184	0.008919
	WAI	0.038631	0.002736	0.003234
	BA	−0.015738	−0.000262	−0.00105
	Distance to green areas	0.113154	0.010995	0.034309
	Constant term	0.780519	0.106907	0.885141
	Log likelihood	−1759.95	3749.93	7799.59
	R2	0.25	0.73	0.81
Type H (n = 10730)	Elevation	0.033696	0.000781	0.002747
	NDVI	0.001823	0.00155	0.00017
	BH	−0.07323	0.00266	0.00045
	WAI	0.057249	0.003143	0.00032
	BA	−0.01682	−0.00106	−0.00032
	Distance to green areas	0.018694	0.001708	0.00559
	Constant term	−0.27792	−0.01038	−0.30435
	Log likelihood	−3502.54	15,245.60	17,207.67
	R2	0.14	0.78	0.78
Type I (n = 8351)	Elevation	0.00788	0.00403	0.00667
	NDVI	0.010434	0.0037	0.00132
	BH	0.133405	0.018523	0.002249
	WAI	−0.08795	−0.00789	−0.00253
	BA	−0.07131	−0.00825	−0.0008
	Distance to green areas	0.045243	0.010169	0.012248
	Constant term	−1.31879	−0.18362	−1.2174
	Log likelihood	−2399.94	6189.14	13,935.50
	R2	0.21	0.71	0.79

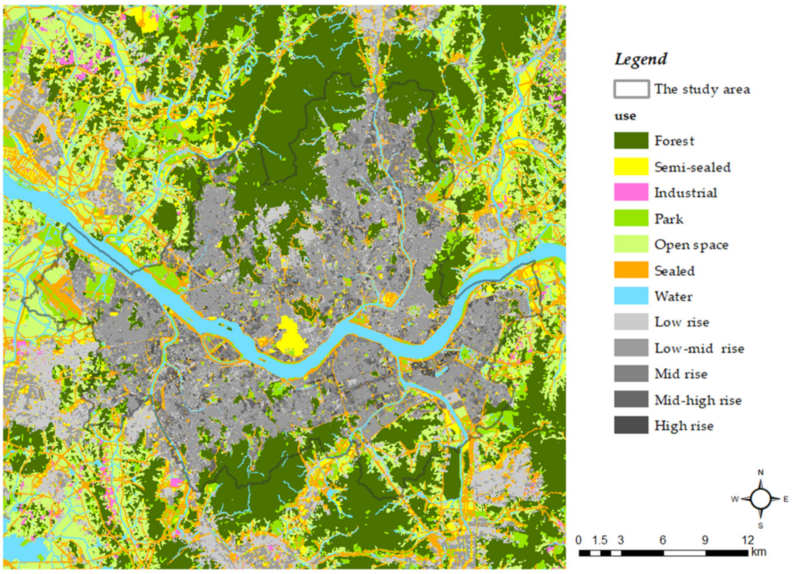

Land use

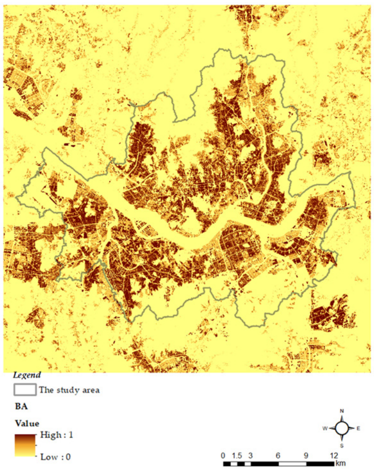

BA

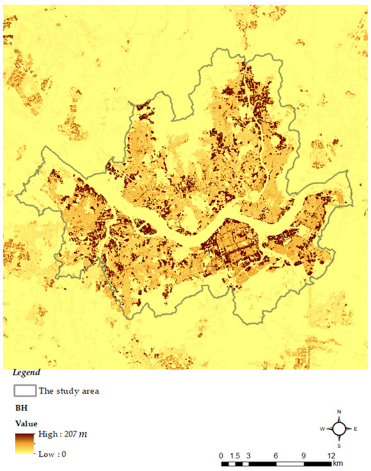

BH

WAI

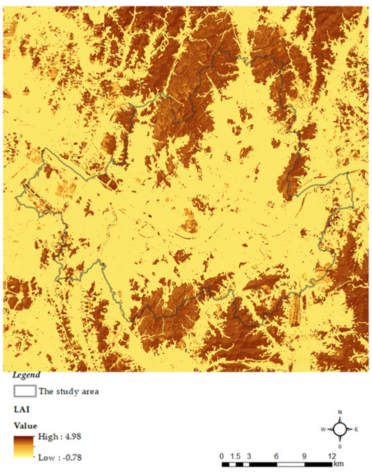

LAI

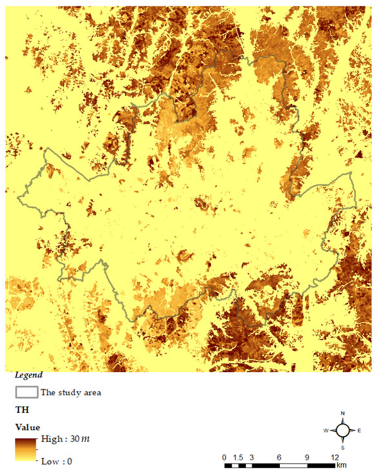

TH

Figure A2. KLAM_21 modeling Physical Parameters results.

References

1. Landsberg, H.E. *The Urban Climate*; Elsevier Science: Amsterdam, The Netherlands, 1981.
2. Rizwan, A.M.; Dennis, L.Y.; Chunho, L. A review on the generation, determination and mitigation of Urban Heat Island. *J. Environ. Sci.* **2008**, *20*, 120–128. [CrossRef] [PubMed]
3. Oke, T.R. Towards better scientific communication in urban climate. *Theor. Appl. Climatol.* **2006**, *84*, 179–190. [CrossRef]
4. Acosta, M.P.; Vahdatikhaki, F.; Santos, J.; Hammad, A.; Dorée, A.G. How to bring UHI to the urban planning table? A data-driven modeling approach. *Sustain. Cities Soc.* **2021**, *71*, 102948. [CrossRef]
5. Parker, J. The Leeds urban heat island and its implications for energy use and thermal comfort. *Energy Build.* **2021**, *235*, 110636. [CrossRef]
6. Ng, E.; Chen, L.; Wang, Y.; Yuan, C. A study on the cooling effects of greening in a high-density city: An experience from Hong Kong. *Build. Environ.* **2012**, *47*, 256–271. [CrossRef]
7. Kwok, Y.T.; de Munck, C.; Lau, K.K.-L.; Ng, E. To what extent can urban ventilation features cool a compact built-up environment during a prolonged heatwave? A mesoscale numerical modelling study for Hong Kong. *Sustain. Cities Soc.* **2022**, *77*, 103541. [CrossRef]
8. Gedzelman, S.D.; Austin, S.; Cermak, R.J.; Stefano, N.; Partridge, S.D.; Quesenberry, S.; Robinson, D.A. Mesoscale aspects of the Urban Heat Island around New York City. *Theor. Appl. Climatol.* **2003**, *75*, 29–42. [CrossRef]
9. Mayer, H. Bestimmung von stadtklimarelevanten Luftleitbahnen. *UVP-Report* **1994**, *5*, 265–267.
10. Priyadarsini, R.; Hien, W.N.; David, C.K.W. Microclimatic modeling of the urban thermal environment of Singapore to mitigate urban heat island. *Sol. Energy* **2008**, *82*, 727–745. [CrossRef]
11. Yim, S.H.L.; Fung, J.C.H.; Ng, E.Y.Y. An assessment indicator for air ventilation and pollutant dispersion potential in an urban canopy with complex natural terrain and significant wind variations. *Atmos. Environ.* **2014**, *94*, 297–306. [CrossRef]
12. Hsieh, C.-M.; Huang, H.-C. Mitigating urban heat islands: A method to identify potential wind corridor for cooling and ventilation. *Comput. Environ. Urban Syst.* **2016**, *57*, 130–143. [CrossRef]
13. Wang, Z.-H.; Li, Q. Thermodynamic characterisation of urban nocturnal cooling. *Heliyon* **2017**, *3*, e00290. [CrossRef] [PubMed]
14. Barlag, A.-B.; Kuttler, W. The significance of country breezes for urban planning. *Energy Build.* **1991**, *15*, 291–297. [CrossRef]
15. Ministerium, F.V.; Baden-Württemberg, I. *Städtebauliche Klimafibel. Hinweise für die Bauleitplanung*; Ministerium für Verkehr und Infrastruktur Baden-Württemberg: Stuttgart, Germany, 2012.
16. Blumen, W.; Grossman, R.; Piper, M. Analysis of heat budget, dissipation and frontogenesis in a shallow density current. *Bound.-Layer Meteorol.* **1999**, *91*, 281–306. [CrossRef]
17. Ingenieure, V.D. Environmental meteorology-local cold air. In *VDI Guideline 3787, Part 5*; Beuth: Berlin, Germany, 2003; Volume 85, pp. 14–29.
18. Sandeepan, B.; Rakesh, P.; Venkatesan, R. Numerical simulation of observed submesoscale plume meandering under nocturnal drainage flow. *Atmos. Environ.* **2013**, *69*, 29–36. [CrossRef]
19. King, E.; Wetterdienst, D. *Untersuchungen über Kleinräumige Änderungen des Kaltluftflusses und der Frostgefährdung durch Strassenbauten: Mit 5 Tab*; Dt. Wetterdienst, Zentralamt: Offenbach, Germany, 1973.
20. Röckle, R.; Richter, C.; Höfl, H.; Steinicke, W.; Streifeneder, M.; Matzarakis, A. *Klimaanalyse Stadt Freiburg*; Auftraggeber Stadtplanungsamt der Stadt Freiburg: Freiburg, Germany, 2003.
21. Pypker, T.; Unsworth, M.H.; Lamb, B.; Allwine, E.; Edburg, S.; Sulzman, E.; Mix, A.; Bond, B. Cold air drainage in a forested valley: Investigating the feasibility of monitoring ecosystem metabolism. *Agric. For. Meteorol.* **2007**, *145*, 149–166. [CrossRef]
22. Sachsen, T.; Ketzler, G.; Knörchen, A.; Schneider, C. Past and future evolution of nighttime urban cooling by suburban cold air drainage in Aachen. *J. Geogr. Soc. Berl.* **2013**, *144*, 274–289.
23. Sievers, U.; Kossmann, M. The cold air drainage model KLAM_21-Model formulation and comparison with observations. *Weather. Clim.* **2016**, *36*, 2–24. [CrossRef]
24. Grunwald, L.; Kossmann, M.; Weber, S. Mapping urban cold-air paths in a Central European city using numerical modelling and geospatial analysis. *Urban Clim.* **2019**, *29*, 100503. [CrossRef]
25. Scherer, D.; Fehrenbach, U.; Beha, H.-D.; Parlow, E. Improved concepts and methods in analysis and evaluation of the urban climate for optimizing urban planning processes. *Atmos. Environ.* **1999**, *33*, 4185–4193. [CrossRef]
26. Katzschner, L. The urban climate as a parameter for urban development. *Energy Build.* **1988**, *11*, 137–147. [CrossRef]
27. Son, J.M.; Eum, J.H.; Kim, D.P.; Kwon, J. Management strategies of thermal environment in urban area using the cooling function of the mountains: A case study of the Honam Jeongmaek areas in South Korea. *Sustainability* **2018**, *10*, 4691. [CrossRef]
28. Gu, K.; Fang, Y.; Qian, Z.; Sun, Z.; Wang, A. Spatial planning for urban ventilation corridors by urban climatology. *Ecosyst. Health Sustain.* **2020**, *6*, 1747946. [CrossRef]
29. He, B.-J. Potentials of meteorological characteristics and synoptic conditions to mitigate urban heat island effects. *Urban Clim.* **2018**, *24*, 26–33. [CrossRef]
30. Lee, D.; Oh, K.; Jung, S. Classifying Urban Climate Zones (UCZs) Based on Spatial Statistical Analyses. *Sustainability* **2019**, *11*, 1915. [CrossRef]
31. Tobler, W.R. A computer movie simulating urban growth in the Detroit region. *Econ. Geogr.* **1970**, *46*, 234–240. [CrossRef]
32. Song, B.; Park, K. Mountain valley cold air flow interactions with urban morphology: A case study of the urban area of Changwon, South Korea. *Landsc. Urban Plan.* **2023**, *233*, 104703. [CrossRef]

33. Son, J.-M.; Eum, J.-H.; Kim, S. Wind corridor planning and management strategies using cold air characteristics: The application in Korean cities. *Sustain. Cities Soc.* **2022**, *77*, 103512. [CrossRef]
34. Grunwald, L.; Schneider, A.-K.; Schroeder, B.; Weber, S. Predicting urban cold-air paths using boosted regression trees. *Landsc. Urban Plan.* **2020**, *201*, 103843. [CrossRef]